Magnetotransport in a doubly connected two-dimensional quantum Hall system in the low magnetic field regime

J. Oswald and M. Oswald
University of Leoben, Institute of Physics, Franz Josef Str. 18, A-8700 Leoben, Austria
(Received 23 June 2006; revised manuscript received 16 August 2006; published 31 October 2006)

In a preceding paper [Phys. Rev. B **72**, 035334 (2005)], experimental results for the so-called "anti-Hall bar within a Hall bar" configuration have been compared with numerical simulations for the high magnetic field regime. The sample structure is a doubly connected, double-boundary electronic system that has been experimentally investigated by Mani. The application of a network model for magnetotransport allows us to evaluate the longitudinal and Hall voltages in this geometry. Thus, within our network model, we rebuild the experimental configuration, including the sample geometry and the two independent floating current sources. In this paper we extend our calculations to the low magnetic field regime, where the quantum Hall effect is not yet established. Like in the high magnetic field regime, we realize the Hall voltages and longitudinal voltages at both the inner and outer boundaries to behave in excellent agreement with Mani's experiments. We find that the Hall voltages at the inner (anti-Hall bar) and outer (Hall bar) boundaries depend just on the individual current injected via the corresponding boundary, while the longitudinal voltage depends exactly on the sum of both injected currents.

DOI: 10.1103/PhysRevB.74.153315 PACS number(s): 73.43.Cd, 73.43.Fj, 73.43.Qt

I. INTRODUCTION

The quantized Hall effect (QHE) stimulated a broad experimental and theoretical study of the two-dimensional electron system that was aimed at understanding the physical origin of this remarkable phenomenon.[1] Laughlin[2] provided an explanation of the observed Hall quantization by carrying out a gedanken gauge argument experiment on a two-dimensional electron system, which is rolled up into a cylinder. The underlying theory suggests a bulk origin for the QHE. Büttiker[3] utilized a Landauer formalism, which considers edge channels (EC's) to play the major role for the quantized Hall effect (see also Refs. 4 and 5).

In order to determine the relative contributions of the bulk and the edge current, Mani developed an experimental configuration that combined aspects of the Hall geometry, which is often investigated in the laboratory, with the doubly connected topology of Laughlin's cylinder.[6–8] Mani's resulting inversion-symmetric "anti-Hall bar within a Hall bar" configuration (see Fig. 1) included a planar doubly connected specimen, with current and voltage contacts on both the interior and exterior boundaries, and a current source attached to each boundary. Despite the topological equivalence with Laughlin's cylinder, currents still have to be injected through edges, while Laughlin was assuming a preexisting bulk current. The role of this bulk current in Mani's experiments is taken by the sum or difference of both injected currents. Thus, Mani performed measurements using two independent floating current sources, one for the exterior boundary "Hall bar" and the other for the interior boundary "anti-Hall bar." The experiments showed dual simultaneous, independent Hall voltages, one at both the inner and outer boundaries of the specimen. The same series of measurements indicated, however, that the longitudinal voltages were proportional to the sum of the currents injected via the two boundaries, and these voltages were identical.[6–8]

We apply a network model in order to reproduce the experimental situation theoretically. For the high magnetic field regime this has been already reported in detail together with a brief introduction to the used network model.[9] Recently, this network model has been extended in order to address also the low field regime of magnetotransport.[10] Thus, we are now in the position to model also the low field regime of Manis experiments, where the Hall effect rises linearly without plateaus. For more details about the network model and the motivation for performing experiments and simulations on this doubly connected geometry, refer to the cited papers.[9,10]

II. RESULTS

The network used for the simulation of the anti-Hall bar within a Hall bar structure is rectangular in shape and consists of 57×41 nodes. Two independent constant current sources $I_{A,B}$ and $I_{1,2}$ are connected to the outer and inner boundaries of the sample as indicated in Fig. 1. Figure 2 shows a snapshot of the used network grid, with dots indicating the nodes of the network. The areas with white dots have a vanishing carrier density, while areas with gray dots indicate the bulk region with a carrier density of $n_0 = 4 \times 10^{11}$ cm^{-2}. Thus, the shape of the sample is defined by the lateral carrier distribution introduced to this network. The width of the annulus (see Fig. 2) in the region of the voltage probes contains nine nodes. The voltage probes, which are labeled from *C* to *F* for the Hall bar and from 3 to 6 for the anti-Hall bar, are four nodes long and five nodes wide. This means that for the simulations in this paper we use a much smaller number of nodes for representing the sample as compared to Ref. 9. This is necessary, because in the low field regime the number of involved Landau levels (LL's) increases enormously as compared to the high field regime. Therefore we would go beyond the limits of our computing capabilities without reducing the number of nodes. Nevertheless, the quality of the obtained simulation data is still very high. An effective mass of $m^* = 0.07$ has

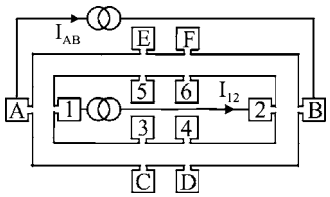

FIG. 1. The "anti-Hall bar within a Hall bar" experimental configuration utilized by Mani (Refs. 6–8). Here, the exterior boundary, associated contacts, and current source $I_{A,B}$ constitute the Hall bar, while the interior boundary, interior contacts, and the current supply $I_{1,2}$ make up the anti-Hall bar configuration. In the typical experiment, each of the floating current sources are set to a constant value, and the voltages on the Hall bar and/or the anti-Hall bar are probed as a function of the ramped transverse magnetic field.

been used for calculating the occupation numbers of the LL's and the self-consistent lateral carrier density profile. The effective g factor has been set to $g_{eff}=5$ in order to demonstrate the set-in of spin splitting already in the regime below 1 T. A magnetic-field-dependent LL broadening was realized with $\Gamma=\Gamma_0 B^{1/2}$ and $\Gamma_0=0.5$ meV/$T^{1/2}$.[11]

The whole set of data was generated in a way that first $I_{A,B}$ was held constant at 20 nA, while between different magnetic field sweeps $I_{1,2}$ has been incremented in steps from $I_{1,2}=-20$ nA to $+20$ nA. Next, $I_{1,2}$ was held constant at -20 nA while between different magnetic field sweeps $I_{A,B}$ has been incremented in steps from $I_{A,B}=-20$ nA to $+20$ nA.

As shown in Fig. 3(a), the Hall voltage $V_{3,5}$ at the inner boundary is proportional to $I_{1,2}$ while it is completely insensitive to the current $I_{A,B}$. In contrast, Fig. 3(b) demonstrates that the Hall voltage $V_{C,E}$ at the outer boundary is proportional to $I_{A,B}$ while it is completely insensitive to the current $I_{1,2}$. The polarity of the Hall voltage $V_{C,E}$ for a current $I_{A,B}$ flowing from left to right via the outer boundary is the same as the polarity of the Hall voltage $V_{3,5}$ for $I_{1,2}$ flowing in the opposite direction via the inner boundary. Remarkably, two different quantized Hall voltages can be observed simultaneously in this configuration, and each depends only on the current injected via the corresponding boundary even in the regime where the Hall plauteaus are not yet established. Figure 4 shows the simulation of the longitudinal voltage at the outer boundary, which appears proportional to the sum of the supplied currents. The longitudinal voltage at the inner boundary is identical within the linewidth to that of the outer boundary and therefore it is not shown separately.

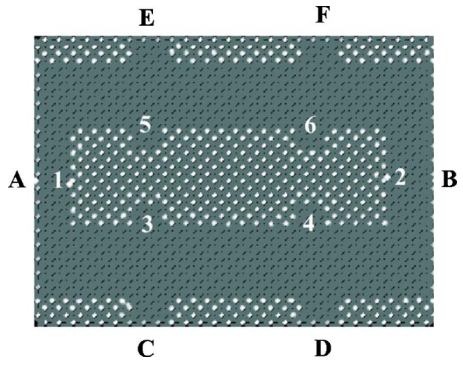

FIG. 2. (Color online) Sample layout for the network model of the "anti-Hall bar within a Hall bar" geometry with two independent current sources $I_{A,B}$ and $I_{1,2}$. The network consists of interconnected nodes, which appear as circles, with the gray scale applied towards indicating the local carrier density. The area with dark nodes indicates a constant carrier concentration of $n_0=4\times10^{11}$ cm^{-2}, which defines the bulk region of the sample. The white dots indicate the carrier-free regions. The positions of the current contacts $(A,B,1,2)$ are indicated at the outer and inner boundaries of the bulk region. The Hall voltages are measured between the voltage probes (3,5) for the anti-Hall bar and between (C,E) for the Hall bar. The corresponding longitudinal voltages are measured between the voltage probes (3,4) for the anti-Hall bar and (C,D) for the Hall bar.

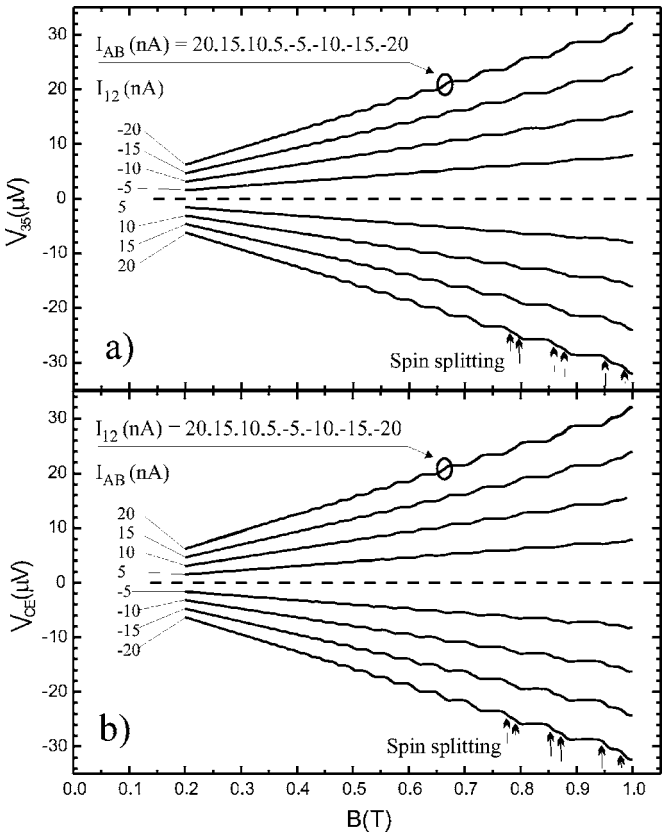

FIG. 3. (a) Simulation of the interior anti-Hall bar Hall voltage $V_{3,5}$ at different currents $I_{1,2}$ and different currents $I_{A,B}$. The interior Hall voltage $V_{3,5}$ is proportional to the interior current $I_{1,2}$, but insensitive to the exterior current $I_{A,B}$. (b) Simulation of the exterior Hall bar Hall voltage $V_{C,E}$ at different interior currents $I_{1,2}$ and different exterior currents $I_{A,B}$. The exterior Hall voltage $V_{C,E}$ is proportional to the exterior current $I_{A,B}$, but insensitive to the interior current $I_{1,2}$. Note that the shape of the traces in (a) and (b) appears identical within the linewidth, but they result from different contact pairs. For the same current direction, the polarity of the Hall voltage at the inner boundary appears reversed as compared to the Hall voltage at the outer boundary.

In experiments, Mani used a GaAs/AlGaAs single heterostructure with a carrier density of $n_0=3\times10^{11}$ cm^{-2} and a mobility $\mu(4.2\ \mathrm{K})=0.3-0.5\times10^6$ cm^2/V s. The experimental results are shown in Figs. 7 and 8 of Ref. 9, and one can see that the trends seen in the Hall effects are in good agree-

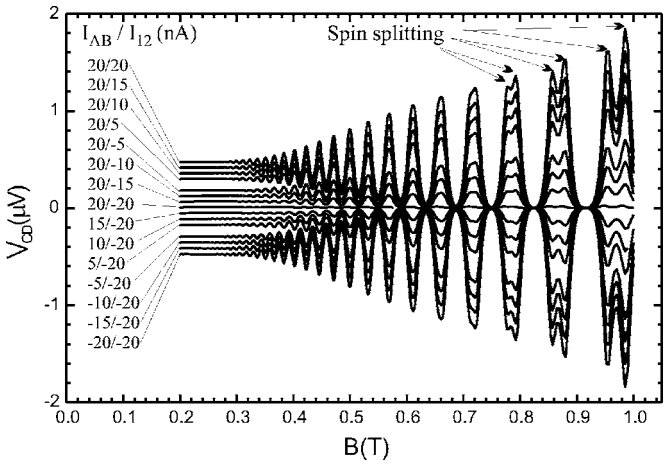

FIG. 4. Simulation of the longitudinal voltage $V_{C,D}$ at the Hall bar at different interior currents $I_{1,2}$ and different exterior currents $I_{A,B}$. Note that this traces are identical within the linewidth with the traces for the longitudinal voltage of the anti-Hall bar; therefore, these are not shown separately.

ment with the trends obtained in the simulations (Fig. 3). As far as the longitudinal voltages are concerned, the simulations (Fig. 4) should be compared with the experimental longitudinal voltage data shown in Fig. 8 of Ref. 9. Simple inspection suggests that there is almost no difference between the longitudinal voltage measured at the outer and inner boundaries in experiment, just as in the simulations.

III. DISCUSSION

The experimental investigation of a doubly connected anti-Hall bar within a Hall bar configuration, which appears topologically equivalent to a doubly connected cylinder, has shown that more than one Hall effect can be realized—and observed—at the same time, in a single specimen.[6–8] For the high magnetic field regime, Mani gave a possible EC-type interpretation of the two independent Hall effects: If EC's are formed, the absence of backscattering separates the two boundaries and helps to realize a situation corresponding to two disconnected samples, with independent Hall effects. Yet Mani also found that in the low magnetic field regime, the samples showed the same boundary-specific Hall effect behavior as in the high magnetic field regime, although EC transport should not yet be established. In addition, the low magnetic field results for the magnetoresistive voltage did not show an exclusive dependence on the current injected into a particular edge; it depended, instead, on the total current injected into the sample. Both the behavior of the Hall voltage and the behavior of the longitudinal voltage are now successfully modeled also for the low magnetic field regime of the not quantized Hall effect, which can be seen as a nontrivial result of our transport model. The parameters used for the simulations are chosen in agreement with those published in a recent paper of Piot *et al.*,[12] who analyzed the enhanced spin splitting in ordinary QHE samples. In order to analyze their data the authors considered the total density of states (DOS) of the LL's to be composed of a Gaussian peak of localized states (width Γ) in which there is embedded a narrower peak (width $\Gamma_{dl}<\Gamma$) of current-carrying delocalized states. In our model (see Ref. 10) the exponent in the coupling function of the nodes corresponds to Γ_{dl} of Piot *et al.* Indeed, using a value like Piot *et al.* of about $\Gamma_{dl}=1.5$ K, we find a set-in of spin splitting in our simulations at about $B=0.75$ T. Piot *et al.* observe the set-in of spin splitting experimentally at about $B=0.5$ T. However, we have used a slightly smaller g factor of $g_{eff}=5$ instead of $g_{eff}=7.7$ of Piot *et al.* Of course, we cannot expect to see these details also in Mani's experiments, because the very high complexity of Mani's sample geometry will not allow for the necessary homogeneity as achievable in our numerical simulations or experimentally in more simple and smaller Hall bar samples. Therefore, for the comparison with Mani's experiments, these details about spin splitting are not relevant, but they demonstrate nicely the potential of our used transport model.

Once again, it appears worth pointing out that on the one hand one obtains two independent Hall voltages (depending only on the current supplied to the corresponding edge) but on the other hand only one longitudinal voltage, which is the same taken either at the outer or inner voltage probe (depending only on the sum of the currents supplied to the outer and inner edges). From this point of view and from the fact that the reported behavior continues also down into the low field regime where Hall plateaus are not yet present, the bulk of the sample seems to contribute homogeneously. We have already shown in Fig. 9 of Ref. 9, that our model indicates bulk current flow also in the plateau regime of the QHE, just as is expected for the low field regime without QHE. From this point of view it seems indeed appropriate to explain the QHE in terms of a bulk effect. However, our model does not distinguish between bulk end edge effects in the first place, and thus it also captures edge-related effects. In this context our model suggests an equivalence between the edge and bulk current picture. This equivalence in the plateau regime is nicely demonstrated for the current-compensated situation ($I_{12}=-I_{AB}$): (i) Using the EC picture, the inner and outer edges appear decoupled and produce independent Hall voltages which have the same value and the same polarity. (ii) Using the bulk current picture, a bulk current flow can be obtained between inner and outer contacts (between A and 1 as well as B and 2, according to Fig. 9 of Ref. 9), but there is no bulk current in the upper and lower branches of the sample. However, the upper and lower branches in this consideration serve as Hall voltage probes for the bulk current shown in Fig. 9 of Ref. 9, giving a Hall voltage between, e.g., C and E but also between 3 and 5, which is the same. While such a behavior appears as trivial for the low field regime, it is evident also for the plateau regime. Thus, our model agrees with both the bulk and edge channel pictures in this case. Such an equivalence has indeed been proposed already earlier (see, e.g., Ruzin and Feng[13]). Nevertheless, edge effects should depend on the sample geometry and, more importantly, on the sample topology. Therefore there should exist a transport regime, where an interplay between edge and bulk is involved. While the bulk region can be considered to contribute homogeneously in both the low and high field regimes, the sample edge introduces some sort of

inhomogeneity. Additionally, the edges behave differently in the low and high field regimes, forming compressible and incompressible stripes at high fields.[14] These may allow a buildup of a disequilibrium between the edge and bulk regions. Therefore, dissipation may not appear just in the bulk due to dissipative bulk current transport, but additionally also due to edge-bulk equilibration. To our opinion, this happens in the regime between QHE plateaus, where edge-bulk equilibration can affect the height of the R_{xx} peaks.[15] Hence, we face the interesting situation that on the one hand the QHE plateaus can be explained either as a pure bulk effect (e.g., Laughlin gedanken experiment) or as a pure edge effect (Büttikers edge channel approach), but on the other hand we believe that also the interplay between edge and bulk may be important.

IV. SUMMARY AND CONCLUSION

We presented simulation results for the low magnetic field regime of the so-called "anti-Hall bar within a Hall bar" configuration, which is a doubly connected two-dimensional plate that is driven simultaneously by two independent floating current sources. These investigations extend the previously published simulations of the same sample configuration[9] to the low magnetic field regime, where Hall plateaus are not yet observed. In full agreement with Mani's experiments, we have demonstrated that one obtains simultaneous independent Hall voltages at the inner ("anti-Hall bar") and outer ("Hall bar") boundaries of the anti-Hall bar within a Hall bar configuration, with each Hall voltage depending exclusively on the current injected into the corresponding boundary. In contrast, the longitudinal voltages are not boundary specific. They depend on the sum of the injected currents and appear identical at the Hall bar and the anti-Hall bar, as demonstrated by experiment and network-model-based numerical simulations. Our theoretical approach can be understood as a generalization of the Landauer-Buttiker formalism for dissipative bulk transport,[10] which now covers edge and bulk effects. Our results support the idea of an equivalence of the edge and bulk current pictures in the plateau regime of the QHE. But we also argue that the regime between plateaus may be affected by an interplay between edge and bulk, meaning that also topological aspects may play a role in this regime. Therefore we conclude that a theoretical approach to the QHE as a whole (plateau regime, but also the regime between plateaus) should also take care of the sample topology.

[1] *The Quantum Hall Effect*, 2nd ed., edited by R. E. Prange and S. M. Girvin (Springer-Verlag, New York, 1990).
[2] R. B. Laughlin, in *The Quantum Hall Effect*, edited by R. E. Prange and S. M. Girvin (Springer-Verlag, New York, 1987), p. 234.
[3] M. Büttiker, Phys. Rev. B **41**, 7906 (1990).
[4] T. Christen and M. Büttiker, Phys. Rev. B **53**, 2064 (1996).
[5] S. Komiyama, O. Astafiev, and T. Machida, Physica E (Amsterdam) **20**, 43 (2003).
[6] R. G. Mani, J. Phys. Soc. Jpn. **65**, 1751 (1996).
[7] R. G. Mani, Europhys. Lett. **34**, 139 (1996).
[8] R. G. Mani, Europhys. Lett. **36**, 203 (1996).
[9] M. Oswald, J. Oswald, and R. G. Mani, Phys. Rev. B **72**, 035334 (2005).
[10] J. Oswald and M. Oswald, J. Phys.: Condens. Matter **18**, R101 (2006).
[11] M. Russ, A. Lorke, D. Reuter, and P. Schafmeister, Physica E (Amsterdam) **22**, 506 (2004).
[12] B. A. Piot, D. K. Maude, M. Henini, Z. R. Wasilewski, K. J. Friedland, R. Hey, K. H. Ploog, A. I. Toropov, R. Airey, and G. Hill, Phys. Rev. B **72**, 245325 (2005).
[13] I. Ruzin and S. Feng, Phys. Rev. Lett. **74**, 154 (1995).
[14] D. B. Chklovskii, B. I. Shklovskii, and L. I. Glazman, Phys. Rev. B **46**, 4026 (1992).
[15] J. Oswald (unpublished).